Blends of Ethylene 1-Octene Copolymer Synthesized by Ziegler–Natta and Metallocene Catalysts. I. Thermal and Mechanical Properties

DIPAK RANA,[1]* KYUCHEOL CHO,[2] TAEWOO WOO,[2] BYUNG H. LEE,[2] SOONJA CHOE[1]

[1] Department of Chemical Engineering, Institute of Polymer Science and Engineering, Inha University, Inchon 402-751, Korea

[2] Taedok Institute of Technology, SK Corporation, Taejon 305-370, Korea

Received 13 November 1998; accepted 2 February 1999

ABSTRACT: The thermal, viscoelastic, and mechanical behaviors of three binary blends of ethylene 1-octene copolymer (EOC) regarding the melt index and density, one component made by Ziegler–Natta (FA and RF in abbreviation of the commercial name) and the other by metallocene catalysts (FM, EN and PL in abbreviation of the commercial name), have been investigated to understand molecular mechanism of the blends. Thermal studies reveal that the two constituents in the three blends exclude one another during crystallization, implying a phase separation. Viscoelastic properties show a single β or γ transition in all the compositions, suggesting a miscibility in the amorphous region. The tensile modulus, yield stress, maximum strength at break, and elongation at break follow the rule of mixtures if the comonomer content does not differ too much. Otherwise, the modulus and yield stress are negatively deviated, whereas elongation at break is positively deviated from the weight-average value. The tensile properties of film at yield and break in the machine direction is increased with an addition of FM in the FA + FM blend. Although all three blends form separate crystals in the crystalline state, a correlation exists between the mechanical properties and the density of EOCs. © 1999 John Wiley & Sons, Inc. J Appl Polym Sci 74: 1169–1177, 1999

Key words: ethylene 1-octene copolymers; Ziegler–Natta and metallocene catalysts

INTRODUCTION

Polyolefins are the volume leader of polymers in the industrial field. A vast amount of blends in linear low-density polyethylene (LLDPE) with conventional polyolefins have been commercially used in the agricultural application and packaging industry as an extrusion-blown film. The processibility in producing blown films of LLDPE blend may be divided into two in terms of extrudability and bubble stability, which can be controlled by the molecular weight, its distribution, and the length of side-chain branching. The bubble stability during the production of blown film is affected by the melt strength of the material. In general, LLDPE contains 1-butene, 1-hexene, or 1-octene comonomer. It is reported that the distribution of comonomer in LLDPE is not possibly controlled by synthesis by using Ziegler–Natta catalyst.[1] Recently, synthesis of LLDPE of which the distribution of comonomer is controlled has been commercialized using metallocene catalyst.[2,3] In the case of the Ziegler–Natta catalyst,

* *Present address:* Polymer Sci. Unit, IACS, Calcutta-32, India.

Correspondence to: S. Choe.

Contract grant sponsor: SK Corporation.

Journal of Applied Polymer Science, Vol. 74, 1169–1177 (1999)

 CCC 0021-8995/99/051169-09

which is multi-site in its nature, heterogeneous distribution of comonomer units results, whereas metallocene catalyst, which is identical to each catalytic site, produces a uniform distribution of comonomer. It is well known that the miscibility of polyolefins is dependent on their chain structures. Although much research has been employed on the polyolefin blends containing LLDPE made by Ziegler–Natta catalyst,[4–10] few have been reported made by metallocene catalyst.[2,3] Thus additional study is needed for the recently developed LLDPE made by metallocene catalyst.

There are many interesting results regarding polyolefin blends in recent literature.[2–20] Blends of ethylene-1-octene elastomer containing a lower percentage of 1-octene comonomer form separate crystals in the crystalline state, whereas solid-state phase behavior in the amorphous region depends on the comonomer content. If the branch concentration of two copolymers is highly different, then the noncrystalline regions are not miscible. The miscibility of the noncrystalline regions produces a synergy effect on the tensile strength.[2,3] Ultra-low density polyethylene (ULDPE) exhibits broad β relaxation at subambient temperature measured by dynamic mechanical analysis and also shows superior low-temperature impact property.[11–13] High and low molecular weights of high-density polyethylene (HDPE) made by metallocene catalyst are found to be miscible themselves by rheological measurements although they are different in molecular weight.[14,15] Blends of HDPE and LLDPE show liquid–liquid phase separation at about 125 and 170°C according to morphological study.[16] The interfacial tension in the polyolefin elastomer is decreased with increased content of 1-octene comonomer.[17] The mechanical properties of LLDPE films are generally influenced by the molecular structure and morphology; both are dependent on the processing conditions.[18–20]

The systematic studies regarding miscibility and processability of LLDPE made by Ziegler–Natta catalyst with other conventional polyolefins have been carried out in this laboratory.[21–24] Our present work continues to examine the thermal, viscoelastic, and mechanical behaviors and molecular mechanism of the blends in ethylene-1-octene copolymers (EOCs) made by Ziegler–Natta and metallocene catalysts. The EOC materials contain three LLDPEs, one very low density polyethylene (VLDPE), and one ULDPE, on the basis of density classification. We prefer to use general terminology, ethylene-1-octene copolymer (EOC) rather than LLDPE, VLDPE, ULDPE, plastomer, or elastomer. The mechanical properties highly depend on the molecular weight, polydispersity index (PDI), comonomer concentration, and its uniformity, which is controlled by the preparation method. The molecular weight and its distribution reflect the melt index (MI) of the polymer; in general, the higher the molecular weight, the lower the MI value is observed. On the other hand, the density (d) of the material depends on the comonomer concentration. We have attempted to mix the EOCs made by Ziegler–Natta and metallocene catalysts in terms of the variation of density and MI to see any relationship between the various properties and the blend systems. The aim of this project is to improve the processing parameter of the film formation in which LLDPE blend is largely used. We have also investigated mechanical and optical properties of blown film.

EXPERIMENTAL

Materials and Blend Preparation

The polymers used in this study are commercial grades. Ziegler–Natta-catalyzed EOCs (abbreviated to Ziegler–Natta EOCs) are the product of SK Corporation, Ulsan, Korea. Metallocene-catalyzed ethylene-1-octene copolymers (abbreviated to metallocene EOCs) are the product of Dow Chemicals, Wilmington, DE, USA. The density, MI, and the comonomer content are provided by the manufacturer and listed in Table I. On the basis of the MI and density, a hybrid of binary blends of EOCs is classified into three categories as listed in Table II. System 1, medium MI and density of both components (MI and density are the same), Ziegler–Natta and metallocene EOCs [the FA + FM system]; System 2, high MI and density of Ziegler–Natta EOC with low MI and density of metallocene EOC [the RF + EN system], and System 3, high MI and density of Ziegler–Natta EOC with high MI and low density of metallocene EOC [the RF + PL system].

Binary systems of Ziegler–Natta and metallocene EOCs were melt blended in proportion to the weight ratio as shown in Table II. Twin-screw extruder (Brabender PL 2000, Duisburg, Germany) was used at a counter-rotating mode with a high mixing condition. The temperature profiles were 190, 200, 210°C for the feed zone, the compression zone, and the metering and die end, re-

Table I Thermal and Molecular Weight Characterization Data of the Base Resin

Catalyst	Brand Name	Grade (abbreviation)	Melting Point T_m (°C)	Crystallization Point T_c (°C)	ΔH_m (J/g)	$-\Delta H_c$ (J/g)	$M_n \times 10^4$	$M_w \times 10^5$	PDI	MI	Density
Metallocene	Engage	8150 (EN)	56.6	38.5	85.6	72.8	14.7	3.19	2.17	0.50	0.868
	Affinity	PL1845 (PL)	105	86.4	113.1	98.7	5.21	1.5	2.88	3.5	0.910
		FM1570 (FM)	111.3	94.7	118.9	107	8.18	2.08	2.54	1.0	0.915
Ziegler–Natta	Yuclair	FA811U (FA)	123.7	104.2	125.1	113	7.82	3.24	4.14	1.0	0.919
		RF500U (RF)	126.8	106.4	135.6	121.2	5.32	1.74	3.26	2.8	0.938

spectively. The screw speed was held at 50 rpm and extruded materials were pelletized after passing through cold water at 25°C. All the pure polymers and blends were processed under the same conditions to give them the identical thermal history. For the blown film properties of FA + FM, two more blend compositions FA/FM, 1 : 3 and 3 : 1, are prepared under the same conditions as mentioned before. All the pure polymers were also processed under the same conditions to give them identical thermal history and blends as well. The resin pellets were melt pressed in a Carver laboratory hot press at 190°C for 5 min under about 2×10^4 Pa and allowed to cool under atmospheric pressure. The specimens were prepared in a desired dimension for the instrumental measurements.

The films were fabricated using Blown Film ϕ50 (Theysohn). The machine specifications are the barrier screw type with a diameter of 50 mm, L/D 24, dual-tip-type air ring, die gap of 2 mm, and its diameter of 150 mm. The processing conditions are the following: Screw speed is 40.2 rpm; line speed is 7.2; the ratio of blown up and draw down are 2.1 and 18.2, respectively. The resin temperature and pressure are 190°C and 242 psi, respectively. The extrusion temperature for cylinder zones C1, C2, C3, the adapter, and dies D1, D2, and D3 are 180, 201, 203, 200, 200, 200, and 200°C, respectively.

Measurements and Instrumental Analysis

Molecular weights of the polymers were measured by Waters GPC 150C at 140°C using 1,2,4-trichlorobenzene as a solvent, and monodisperse molecular weight polystyrene was used as a standard. The number-average molecular weight (M_n), weight-average molecular weight (M_w), and PDI (M_w/M_n) were calculated from the GPC curves. The molecular weight data of the polymers are listed in Table I.

Melting and crystallization behaviors of the blends were measured by a Perkin–Elmer DSC-7. Indium and zinc were used for the calibration of the melting temperature and the enthalpy of fusion. The samples were scanned up to 180°C at a heating rate of 10°C/min, annealed for 5 min, and cooled down to 50°C at a cooling rate of 10°C/min. Then the same samples were rescanned at the same rate and temperature interval. For pure EN as a special case, the cooling temperature was 0°C, but other parameters were identical. The melting temperature (T_m), crystallization tem-

Table II Composition of Hybrid Resin

System	Specification	Ziegler–Natta		Metallocene		Calculated Density	Calculated MI
1	Medium MI & d	FA	90	FM	10	0.9186	1.0
	and		70		30	0.9178	1.0
	Medium MI & d		50		50	0.9170	1.0
			20		80	0.9158	1.0
2	High MI & d	RF	90	EN	10	0.9310	2.3569
	and		70		30	0.9170	1.6699
	Low MI & d		50		50	0.9030	1.1832
			30		70	0.8890	0.8383
			10		90	0.8750	0.5940
3	High MI & d	RF	90	PL	10	0.9352	2.8632
	and		50		50	0.9240	3.1305
	High MI, Low d		10		90	0.9128	3.4228

perature (T_c), heat of fusion (ΔH_m), and heat of crystallization (ΔH_c) were obtained from the second scan of the DSC thermogram. The thermal characterization data of the pure polymers are also shown in Table I.

The viscoelastic properties were measured by using the Polymer Laboratories DMTA Mk III in the range of -145°C to T_m -10°C, and the tensile mode was applied at a constant frequency of 1 Hz at a heating rate of 2°C/min. The relaxational α, β, and γ behaviors were analyzed from the tensile storage modulus E', the tensile loss modulus E'', and the tan δ peaks. All the specimens were rectangular shaped in 10-mm-gauge length, 5-mm width, and 0.5-mm thickness.

The mechanical properties were measured using universal testing machine Instron 4465 with a crosshead speed of 200 mm/min and at ambient temperature. All the specimens were dumbbell-shaped in 25-mm-gauge length, 6-mm width, and 1.6-mm thickness. Mean averages of the different tensile parameters were obtained from the five specimens of each sample.

The mechanical properties of the films, tensile strength at yield and break, and elongation at yield and break were measured by Instron universal testing machine (Model 4301) according to ASTM D 638-91[25] after leaving at 23°C, 50% humidity for 48 h. The dimensions of the test specimens were type IV in ASTM D 638 and the crosshead speed was 200 mm/min. The tear resistance properties were measured in two steps, initial tear strength and Elmendorf (or propagation) tear strength. The first step (i.e., initial tear strength) was measured by Instron (Model 4301) according to the ASTM D 1004-90.[26] The crosshead speed was 500 mm/min. The second step (i.e., propagation tear strength) was measured by a Toyoseiki instrument according to the ASTM D 1922-89[27] test method. The specimen was rectangular type. The falling dart impact strength was measured in the instrument CSI (Model CS126TE-1280) according to the ASTM D 1792-80[28] test method and falling height was 660 mm.

The optical properties, haze, and gloss of the films were measured. The haze of the internal film was measured by Nippon Denshok (Model 300A) using ASTM D 1003-92.[29] The gloss of the film surface was measured using gloss meter (Pacific Scientific, Glossgard II) according to the ASTM D2457-97[30] test method. The beam axis angle used was 45°.

RESULTS AND DISCUSSION

Thermal Behavior

In our present EOC systems, DSC measurement indicates that all of the blends are immiscible in crystalline phase because two distinct melting points corresponding to those of the constituents are observed. The melting behaviors of the blends are drawn in Figure 1(a–c). The T_m of Ziegler–Natta EOC was broadened and started to separate into two T_m's from the composition of 50% metallocene EOC, whereas the T_m of metallocene EOC was broadened and lowered as the metallocene content decreased. The high percentage of the latter component (EOC made by metallocene catalyst) as well as the increased comonomer content in EOC is characterized by a high percentage of amorphous phase. This phenomenon suggests hindering the chain folding of the other compo-

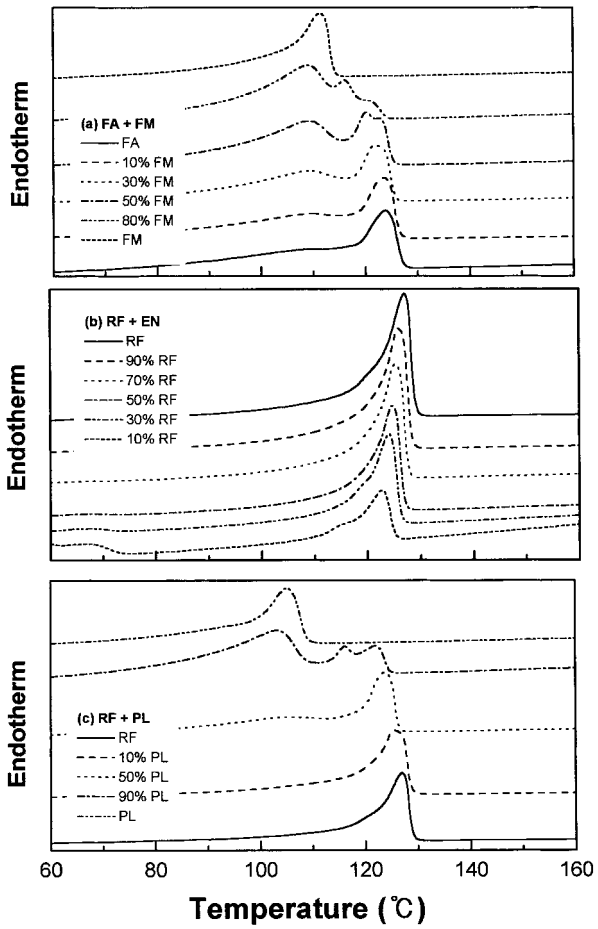

Figure 1 Melting behavior of (a) FA + FM, (b) RF + EN, and (c) RF + PL systems in the second scan of DSC thermogram. The number indicates the percentage of the second component (metallocene-catalyzed EOC) in the blends.

nent of EOC prepared by Ziegler–Natta catalyst into the growing crystal lamella. The crystallization peaks of all the blends are shown in Figure 2(a–c). A double or broadened crystallization peak is observed for the entire blend compositions. In particular, the crystallization peak is shifted toward low temperature as the portion of metallocene EOC increases; this may have arisen from the metallocene EOC acting as a polymeric diluent. The T_c of the Ziegler–Natta EOC always shows a strong single peak, whereas that of the metallocene EOC appeared much weaker and broader.

In the case of System 1 (FA + FM), although it is expected to form a cocrystallization in the crystalline state, the result based on the observed T_m and T_c represents that each component excludes one another during crystallization. This is rather surprising because each constituent in the blend has similar MI, density, chemical structure, and comonomer content except the preparation method of EOC, either Ziegler–Natta or metallocene catalyst. Metallocene EOC is reported to contain long- and short-side chain branching, similar to conventional low-density polyethylene (LDPE), whereas the Ziegler–Natta EOCs show similar characteristics to LLDPE. The thermal study of LLDPE blend with LDPE reported a formation of separate crystals in the crystalline state but miscibility in the amorphous state.[23] Hence the comonomer distribution or the length of the side-chain branching is presumed to be an important factor for the EOC blend to form cocrystals. Recently, the interaction parameter between the polyolefin component has been directly calculated

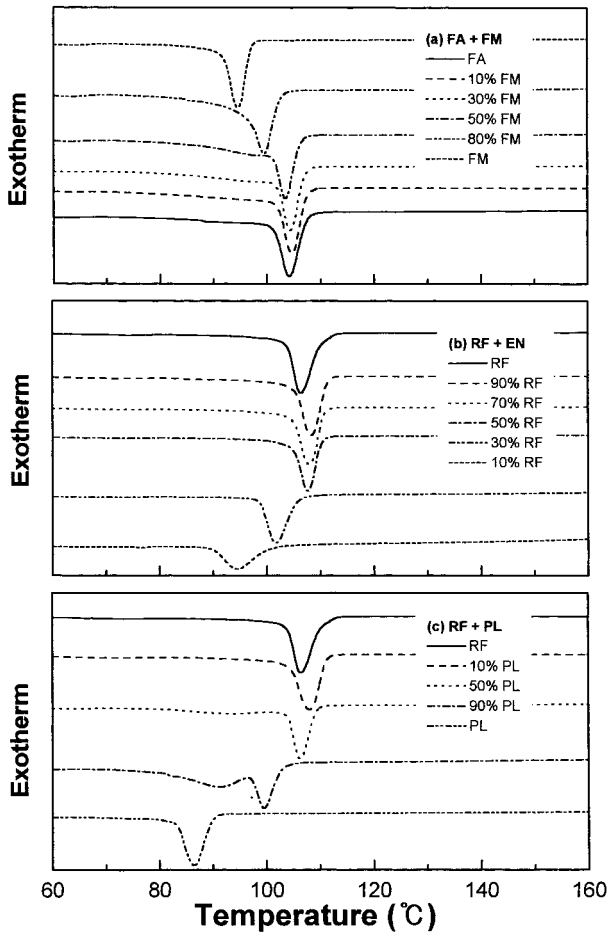

Figure 2 Crystallization behavior of (a) FA + FM, (b) RF + EN, and (c) RF + PL systems in the second scan of DSC thermogram. The number indicates the percentage of the second component (metallocene-catalyzed EOC) in the blends.

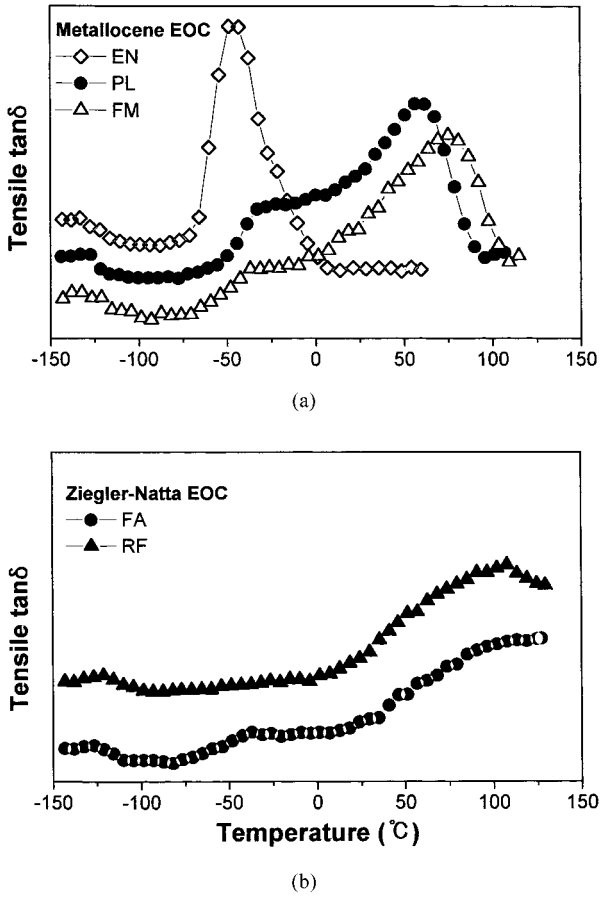

Figure 3 DMTA thermograms of the (a) metallocene and (b) Ziegler–Natta catalyzed EOCs.

using various techniques.[31] The interaction parameter in the System 1 is presumed to be less positive than in System 2 (RF + EN) or System 3 (RF + PL), which is currently under investigation. Pioneering work of ethylene-1-octene elastomeric blends by Bensason et al.[3] concluded that the elastomeric components formed separate crystalline phases according to their experimental and calculated crystallinity data.

Viscoelastic Behavior

In Figure 3(a, b), the DMTA thermograms of the metallocene and Ziegler–Natta EOCs are plotted in the temperature range of −150 and 150°C, respectively. In Figure 3(a), EN shows the β transition at about −45°C and the γ relaxation at −133°C. For PL and FM, the common feature is the observation of the relaxational α, β, and γ peaks where the α transition is at about 56 and 75°C, the β transition is at about −33 and −31°C, and the γ transition is at about −133 and −132°C, respectively. The β relaxation was broadened and shifted to a lower temperature, and the intensity of it was augmented with an increasing concentration of comonomer content. This is in good agreement with reports that the β transition correlates with the concentration of the comonomer content.[23,32,33] The intensity and the position of the β transition are also reported to correlate to a degree of crystallinity or amorphous content. On the other hand, for the Ziegler–Natta resins with FA and RF drawn in Figure 3(b), the broad transitions around 90°C would be related to the melting points of the components. The β relaxation is observed at about −37°C in FA; however, these are hardly observable for RF.

The representative relaxational behavior for System 1, FA + FM, is depicted in Figure 4. In this figure, the single transition between the maximum β peak of FA at −37°C and that of FM at −31°C is observed and then shifted, thereby a miscibility is suggested in the amorphous phase. A similar trend is observed for the rest of the two blends.

Mechanical Property

The representative stress–strain curve for the RF + PL blend is depicted in Figure 5. RF, PL, and all the blend compositions show the yield behavior, followed by the necking with strain softening. In addition, both the modulus (the initial slope in the stress–strain curve) and yield stress decrease as the metallocene EOC content increases. The blend with 90% PL and the pure PL show about 1300% of elongation.

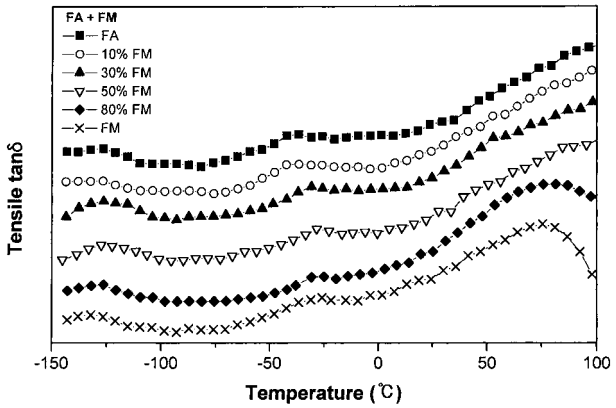

Figure 4 A representative tensile tan δ spectra of System 1, FA + FM. The number indicates the percentage of the second component (metallocene-catalyzed EOC) in the blends.

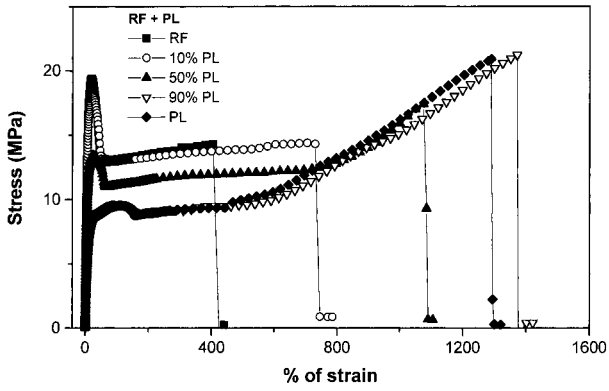

Figure 5 A representative stress–strain curve for RF + PL system. The number indicates the percentage of the second component in the blends.

The mechanical properties, including modulus, yield stress, tensile strength at break, and elongation at break, are analyzed from the stress–strain curves for three blends (System 1, 2, and 3) and shown in Figures 6–8, respectively. There are two distinctive features observed. In Figure 6(a) for System 1 where the comonomer concentration, MI, and density are almost the same, the modulus and yield stress followed the rule of mixtures between the pure polymers and the blends. In addition, synergy effect for the blends with 10 and 30% of FM was obtained. On the other hand, for the rest of the blends (Systems 2 and 3), where the MI and density are much different, the modulus and yield stress decreased with the metallocene component, whereas the tensile strength and elongation at break increased. For RF + EN (System 2), where the difference in comonomer concentration is very large, both the modulus and yield stress are negatively deviated from the weight additive value, whereas the tensile maximum strength at break is positively deviated from the weight average. If the difference in comonomer concentration is not so high, as in the case of System 3 (RF + PL), the tensile modulus, yield stress, maximum strength at break, and elongation at break would follow the rule of mixtures. The same conclusion was reported by Bensason et al.[3] regarding the ethylene-1-octene elastomeric blends. If the comonomer content of two elastomeric components is much different, the tensile properties have not obeyed the weight averages of

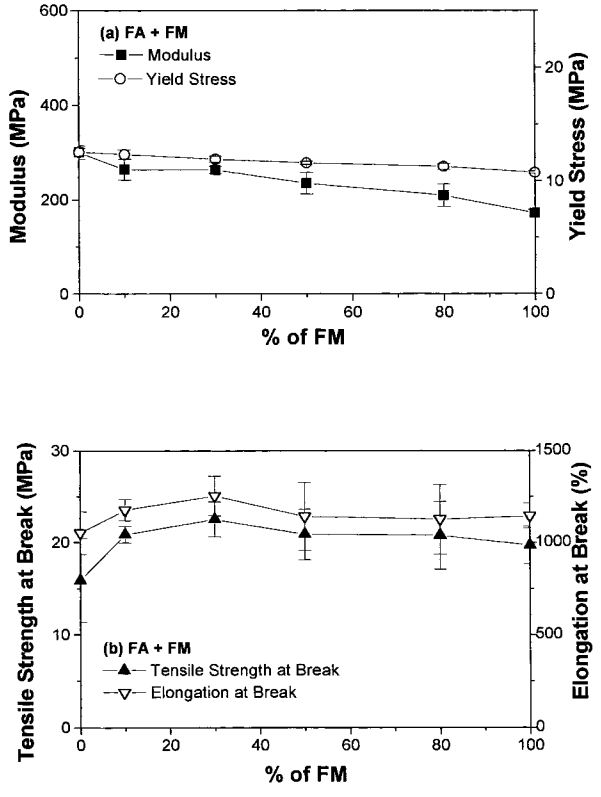

Figure 6 Variation of (a) modulus (■) and yield stress (○), and (b) maximum strength at break (▲) and elongation at break (▽) for FA + FM system.

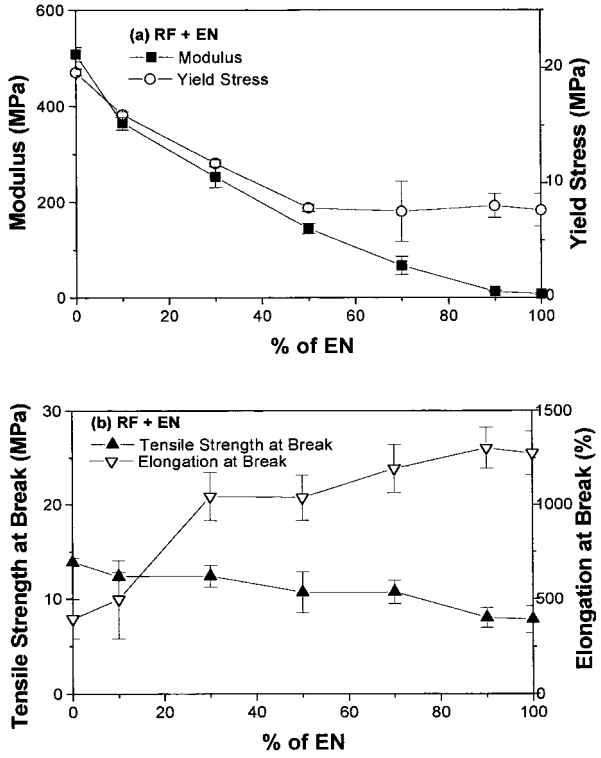

Figure 7 Variation of (a) modulus (■) and yield stress (○), and (b) maximum strength at break (▲) and elongation at break (▽) for RF + EN system.

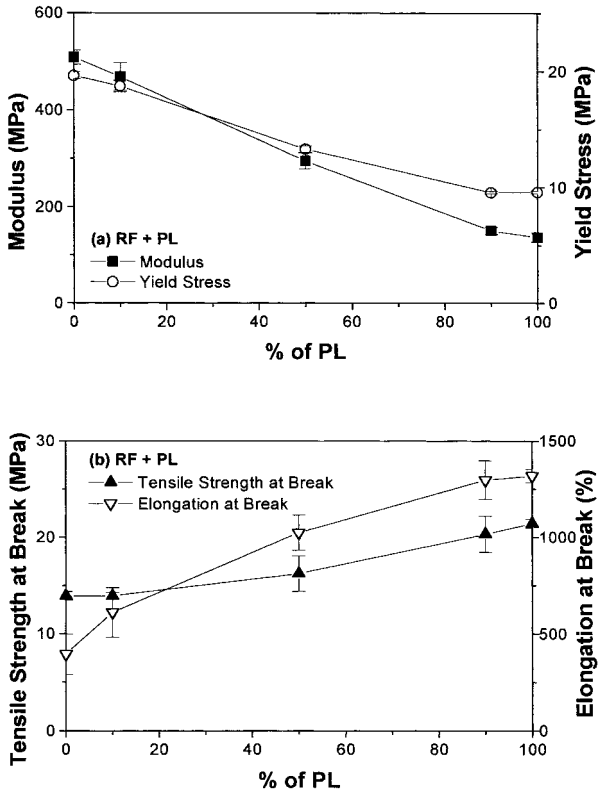

Figure 8 Variation of (a) modulus (■) and yield stress (○), and (b) maximum strength at break (▲) and elongation at break (▽) for RF + PL system.

the pure components. Our results agree well with the claim of Bensason et al.[3]

Mechanical and Optical Properties of Films

The mechanical and optical properties of the blends as well as pure resin films in System 1 are listed in Table III. The tensile property of the film specimen was measured in two directions, machine direction (MD) and transverse direction (TD). It is well known that the mechanical properties of films depend on the molecular arrangement (i.e., the crystalline morphology, molecular orientation, and relaxation process of both the crystalline and amorphous regions). For the preferential orientation of crystal structure, the mechanical strength to the MD is observed to be higher than the TD. It is noted that initial tear strength in MD is higher than the TD. However, the propagation tear strength in MD is lower than the TD. The mechanism of tear propagation is definitely different from the tear initiation. In the case of the optical properties, the degree of internal haze is decreased and the gloss at surface is increased. This result is consistent with the apparently observed transparent film.

To correlate the relationship between the tensile properties and the density, all the tensile data for the pure resins as well as the blends are plotted in a semilog scale as a function of density. The elastic modulus is significantly varied, whereas the yield stress is slightly increased with density. On the other hand, the tensile strength at break is slightly decreased, whereas the elongation at break was slightly increased with density.

CONCLUSIONS

The relationship between both the MI and density of Ziegler–Natta and metallocene EOC blends has been investigated in terms of thermal, viscoelas-

Table III The Mechanical and Optical Characterization Data of the Film

Sample		FA	25% FM	50% FM	75% FM	FM
Tensile strength at break (kg/cm^2)	MD	574	550	529	536	510
	TD	567	543	527	532	495
Tensile strength at yield (kg/cm^2)	MD	125	127	122	122	126
	TD	136	136	127	120	113
Elongation at break (%)	MD	760	699	696	682	637
	TD	804	784	770	761	721
Elongation at yield (%)	MD	17.4	17.5	23.8	25.1	26.1
	TD	15.4	16.7	15.8	13.1	14.3
Initial tear strenght (kg/cm)	MD	110	113	111	109	107
	TD	107	112	96.2	97.5	92.6
Elmendorf tear strength (g/μm)	MD	17.9	14.1	12.6	12.1	10.0
	TD	20.5	23.1	23.2	21.2	18.8
Dart impact (g)		270	350	365	410	515
Haze (%)		19.6	12.2	9.5	7.3	5.6
Gloss (%)		39	63	61	69	75

tic, and mechanical properties. The melting and crystallization behaviors indicate that all the blends form separate crystals, whereas dynamic mechanical thermal analyzer studies show a possibility of miscibility in the amorphous regions regardless of the MI and density. If the comonomer content is not too large, the mechanical properties such as yield stress, modulus, tensile stress at break, or elongation at break relatively follow the rule of mixtures, whereas for highly different comonomer content, negative or positive deviation from the weight-average value was observed. With increasing density, both modulus and yield stress increase, whereas the maximum strength at break and elongation at break have a maximum value at optimum density. Hence, a correlation exists between the mechanical properties and the density of Ziegler–Natta and metallocene EOC blends. In the investigation of the film properties of FA + FM, the tensile strength and the elongation at yield and break are higher in MD than in TD with an incorporation of FM, whereas inverse behavior is observed in the Elmendorf tear strength.

System 1, which shows separate crystals regardless of similar MI, density, and comonomer content, needs further investigation to elucidate the fact. The melt rheology and morphological studies of the blend using scanning electron microscope (SEM) under various techniques such as, after tensile fractured, microtomed cutting at low temperature then etching the amorphous portion, etc., will be disclosed shortly.

Financial support from SK Corporation is gratefully appreciated.

REFERENCES

1. Donatelli, A. A. J Appl Polym Sci 1979, 23, 3071.
2. Bensason, S.; Minick, J.; Moet, A.; Chum, S.; Hiltner, A.; Baer, E. J Polym Sci Polym Phys Ed 1996, 34, 1301.
3. Bensason, S.; Nazarenko, S.; Chum, S.; Hiltner, A.; Baer, E. Polymer 1997, 38, 3513; Polymer 1997, 38, 3913.
4. Donatelli, A. A. J Appl Polym Sci 1979, 23, 3071.
5. Hu, S. R.; Kyu, T.; Stein, R. S. J Polym Sci, Polym Phys Ed 1987, 25, 71; Kyu, T.; Hu, S. R.; Stein, R. S. J Polym Sci, Polym Phys Ed 1987, 25, 89.
6. Ree, M.; Kyu, T.; Stein, R. S. J Polym Sci, Polym Phys Ed 1987, 25, 105.
7. Mirabella, F. M.; Westphal, S. P.; Fernando, P. L.; Ford, E. A.; Williams, J. G. J Polym Sci, Polym Phys Ed 1987, 26, 1995.
8. Hay, J. N.; Zhou, X.-Q. Polymer 1993, 34, 2282.
9. Gupta, A. K.; Rana, S. K.; Deopura, B. L. J Appl Polym Sci 1992, 44, 719; J Appl Polym Sci 1993, 49, 477; J Appl Polym Sci 1994, 51, 231.
10. Tashiro, K.; Izuchi, M.; Kobayashi, M.; Stein, R. S. Macromolecules 1994, 27, 1221; Macromolecules 1994, 27, 1228; Macromolecules 1994, 27, 1234.
11. Dharmarajan, N. R.; Yu, T. C. Plastics Eng 1996, 52, 33.
12. Woo, L.; Ling, M. T. K.; Westphal, S. P. Thermochim Acta 1996, 272, 171.
13. Westphal, S. P.; Ling, M. T. K.; Woo, L. Thermochim Acta 1996, 272, 181.
14. Vega, J. F.; Munoz-Escalona, A.; Santamaria, A.; Munoz, M. E.; Lafuente, P. Macromolecules 1996, 29, 960.
15. Munoz-Escalona, A.; Lafuente, P.; Vega, J. F.; Munoz, M. E.; Santamaria, A. Polymer 1997, 38, 589.
16. Hill, M. J.; Barham, P. J. Polymer 1997, 38, 5595.
17. Carriere, J.; Craig Silvis, H. J Appl Polym Sci 1997, 66, 1175.
18. Patel, R. M.; Butler, T. I.; Walton, K. L.; Knight, G. M. Polym Eng Sci 1994, 34, 1506.
19. Kim, Y. M.; Park, J. K. J Appl Polym Sci 1996, 61, 2315.
20. Abraham, D.; George, K. E.; Joseph Francis, D. J Appl Polym Sci 1998, 67, 789.
21. Cho, K.; Ahn, T. K.; Lee, B. H.; Choe, S. J Appl Polym Sci 1997, 63, 1265.
22. Cho, K.; Ahn, T. K.; Park, I.; Lee, B. H.; Choe, S. J Ind Eng Chem 1997, 3, 147.
23. Lee, H.; Cho, K.; Ahn, T. K.; Choe, S.; Kim, I. J.; Park, I.; Lee, B. H. J Polym Sci, Polym Phys Ed 1997, 35, 1633.
24. Rana, D.; Lee, C. H.; Cho, K.; Lee, B. H.; Choe, S. J Appl Polym Sci 1998, 69, 2441.
25. ASTM D 638. Ann Book ASTM Stand 1991, Vol. 08.01.
26. ASTM D 1004. Ann Book ASTM Stand 1990, Vol. 08.01.
27. ASTM D 1922. Ann Book ASTM Stand 1989, Vol. 08.01.
28. ASTM D 1792. Ann Book ASTM Stand 1980, Vol. 08.01.
29. ASTM D 1003. Ann Book ASTM Stand 1992, Vol. 08.01.
30. ASTM D 2457. Ann Book ASTM Stand 1997, Vol. 08.02.
31. Alamo, R. G.; Graessley, W. W.; Krishnamoorti, R.; Lohse, D. J.; Londono, J. D.; Mandelkern, L.; Stehling, F. C.; Wignall, G. D. Macromolecules 1997, 30, 561.
32. Popli, R.; Glotin, M.; Mandelkern, L.; Benson, R. S. J Polym Sci, Polym Phys Ed 1984, 22, 407.
33. Boyd, R. H. Polymer 1985, 26, 323; Polymer 1985, 26, 1123.